ELSEVIER

www.elsevier.nl/locate/jorganchem

Journal of Organometallic Chemistry 602 (2000) 137–143

Journal of Organo metallic Chemistry

Iridium carbonyl cluster complexes with bidentate phosphine ligands; the X-ray crystal structure of $[Ir_4(CO)_8(dppa)_2]\cdot 3(THF)$

Nagwa Nawar *

Department of Chemistry, Faculty of Science, Mansoura University, PO Box 79, Mansoura 35516, Egypt

Received 26 January 2000; received in revised form 20 February 2000

Abstract

Reactions of $[Ir_4(CO)_{12}]$ with 1,1-bis(diphenylphosphino)ethene, $Ph_2PC(=CH_2)PPh_2$ (dppen) and 1,1-bis(diphenylphosphino)amine, $Ph_2PN(H)PPh_2$(dppa) gave $[Ir_4(CO)_{12-n}(L)_{n-2}]$ (L = dppen or dppa and $n = 2$ or 4) depending upon the reaction conditions. The structures of the cluster complexes are discussed on the basis of IR, ^{31}P-NMR spectroscopic data and FAB mass spectra. The structure of the disubstituted species $[Ir_4(CO)_8(dppa)_2]\cdot 3(THF)$ (THF = tetrahydrofuran, C_4H_8O) has been determined by X-ray crystallography. © 2000 Elsevier Science S.A. All rights reserved.

Keywords: Iridium; Carbonyl; Cluster complexes; bis(Diphenylphosphino)ethene complexes; bis(Diphenylphosphino)amine complexes

1. Introduction

In last two decades there has been a great deal of interest in the preparation and properties of transition metal cluster carbonyl complexes stabilized with multidentate ligands [1–10]. It has been shown that the presence of bridging or capping ligands can increase the stability of the metal atom framework [5] and thus provide useful compounds for the study of catalysis by cluster complexes [11–15]. Compared with the vast body of data accumulated on diphosphines in which the phosphorus nuclei are linked by a carbon atom or chain [8], less has appeared on ligands where the backbone of the molecule comprises a heteroatom or group [16]. In this respect, diphosphines, where the phosphorus nuclei are connected by nitrogen atom, have received little coverage. The only example existing in the literature of a cluster complex stabilized by bis(-diphenylphosphino)amine, $Ph_2PN(H)PPh_2$(dppa), is the silver halide cluster complex [16,17]. In this respect dppa has received our attention because dppen and dppa have shared features in the formation and stabilization of cluster complexes. The X-ray crystal structure of the disubstituted species $[Ir_4(CO)_8(dppa)_2]\cdot 3(THF)$ was determined.

* Fax: +20-50-346781/353584.
E-mail address: sinfac@mum.mans.eun.eg (N. Nawar)

2. Results and discussion

Our attention has been centered on substitution reactions involving loss of carbon monoxide from the tetranuclear metal carbonyl cluster $[Ir_4(CO)_{12}]$ by the bidentate phosphine ligands dppen and dppa. In spite of the cluster carbonyl, $[Ir_4(CO)_{12}]$ is generally considered to be rather unreactive and has an all-terminal CO ligand structure, we find that $[Ir_4(CO)_{12}]$ reacts with equimolar amounts of dppen or dppa to give $[Ir_4(CO)_8(dppen)_2]$ or $[Ir_4(CO)_8(dppa)_2]$ in good yield. Since the substitution of more than two carbonyl ligands is kinetically favored in this reaction [18], the derivative $[Ir_4(CO)_{10}(dppa)]$ or $[Ir_4(CO)_{10}(dppa)]$ cannot be prepared by this route. Instead, we used the method of Stuntz and Shapley [19], which leads to $[Ir_4(CO)_{11}L]$ and $[Ir_4(CO)_{10}L_2]$ (L = monodentate tertiary phosphine) derivatives. Thus, the reaction of $[Ir(CO)_2Cl(p$-toluidine)] with dppen or dppa ligands in the presence of zinc metal and under CO pressure gives a mixture of $[Ir_4(CO)_{10}(dppen)]$ (**1**) and $[Ir_4(CO)_8(dppen)_2]$ (**2**) or $[Ir_4(CO)_{10}(dppa)]$ (**3**) and $[Ir_4(CO)_8(dppa)_2]$ (**4**). The mono- and disubstituted cluster complexes can be separated by a florisil column chromatography. The IR spectra of these iridium derivatives are very similar to the analogous $[Ir_4(CO)_{10}(dppm)]$ and $[Ir_4(CO)_8(dppm)_2]$ complexes (Table 1) [20] in which its dppm ligand

PII: S0022-328X(00)00140-6

adopts a bridging mode. Further support is provided by the fact that the IR spectrum of $[Ir_4(CO)_{10}(diars)]$ (diars = 1,2-bis(dimethylarsino)benzene) (ν(CO): 2071 m, 2038 s, 2026 w, 2001 m, 1996 w, 1847 vw, br, 1805 w, br) [21], in which the diars ligand is coordinated in a chelating mode to one iridium atom, is quite different from the dppen or dppa derivatives reported here or dppm [20]. However, the chemical shifts observed in the ^{31}P-NMR spectra of $[Ir_4(CO)_{10}(dppen)]$ (**1**), $[Ir_4(CO)_8(dppen)_2]$ (**2**), $[Ir_4(CO)_{10}(dppa)]$ (**3**) and $[Ir_4(CO)_8(dppa)_2]$ (**4**) (Table 1) suggest that in all complexes the phosphorus atoms are involved in a five-membered rings and therefore that the dppen or dppa ligands are coordinated in a chelating mode to two iridium atoms. Also, the IR stretching frequencies of 1825 and 1778 cm^{-1} indicated the presence of bridging carbonyls in the $[Ir_4(CO)_{10}(dppen)]$ (**1**) or $[Ir_4(CO)_{10}(dppa)]$ (**3**). Further support for this conclusion is provided by the ^{31}P-NMR spectra of $[Ir_4(CO)_{10}(dppen)]$ (**1**) or $[Ir_4(CO)_{10}(dppa)]$ (**3**) (Table 1). The chemical shifts observed in the ^{31}P-NMR spectra of **1** and **3** (Table 1) suggest that in both complexes the phosphorus atoms are involved in a five-membered ring and therefore the dppen and dppa ligands are coordinated in a bridging mode. Since only a singlet resonance at -17.0 ppm for **1** or -18.1 ppm for **3** were observed on the ^{31}P-NMR spectrum, the two phosphorus atoms in $[Ir_4(CO)_{10}(dppen)]$ or $[Ir_4(CO)_{10}(dppa)]$ are equivalent and coordinated to two iridium atoms in basal plane of the tetrahedron. This suggests that the iridium complexes are structurally quite similar to that reported with dppm derivatives [22] and adopts a bridging coordination mode in the diaxial sites of the basal plane of iridium metals framework.

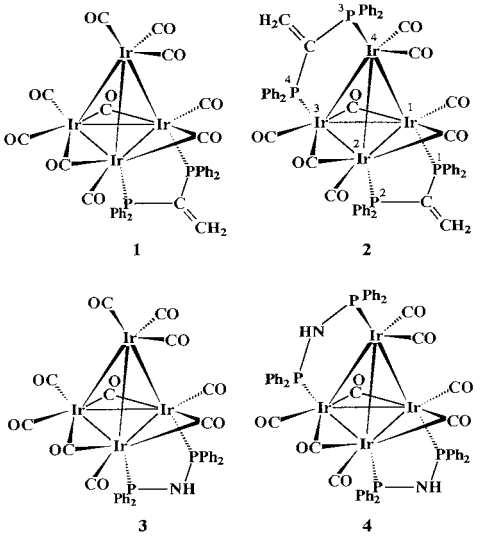

Analysis by FAB mass spectroscopy of $[Ir_4(CO)_{10}(dppen)]$ (**1**) or $[Ir_4(CO)_{10}(dppa)]$ (**3**) gave a parent ion at the desired positions: m/z 1445 for **1** or m/z 1435 for **3**. The fragmentation of **1** or **3** occurs mainly via initial loss of a carbonyl group. The stepwise losses of ten carbonyl groups are observed. Unfortunately, we have not succeeded in isolating good single crystal for **1** or **3**.

$[Ir_4(CO)_8(dppen)_2]$ (**2**) and $[Ir_4(CO)_8(dppa)_2]$ (**4**) were characterized by microanalysis, IR and ^{31}P-NMR spectroscopic data (Table 1). The IR stretching frequencies, 1780, 1765 and 1830 cm^{-1} are due to bridging carbonyl ligands, the rest being due to five terminal carbonyls. Two broad peaks at -19.5 and -42.5 ppm for **2** and 0.3 and -12.4 ppm for **4** were observed in the ^{31}P-

Table 1
Infrared and ^{31}P-NMR data

Complex	ν(CO) (cm^{-1}) [a]	^{31}P-NMR [b]
$[Ir_4(CO)_{10}(dppm)]$	2071 s, 2041 m, 2012 s, 1985m (sh), 1860 w, 1826 m, 1790 m.	-52.3 (s) (at 25 and -95°C)
$[Ir_4(CO)_8(dppm)_2]$	2007 s, 1974 s(br), 1957 s, 1832 vw, 1783 m, 1762 m.	-49.4 (br, s) (at 25°C); -23.5 (P_1) (d, $J(P_1–P_4)$ 42); -44.85 (P_2) (dd, $J(P_2–P_3)$ 48), $J(P_2–P_4)$ 101); -49.8 (P_3) (d, $J(P_3–P_2)$ 48), -61.5 (P_4) (dd, $J(P_4–P_1)$; 42, $J(P_4–P_2)$ 101) (at -95°C).
dppen		-3.4 (s)
$[Ir_4(CO)_{10}(dppen)]$ (**1**)	2070 vs, 2040 s, 2011 vs, 1980 w, 1860 vw, 1825 m, 1778 m.	-18.1 (s) (at 25 and -95°C)
$[Ir_4(CO)_8(dppen)_2]$ (**2**)	2009 s, 1975 vs(br), 1950 w, 1830 w, 1780 m, 1765 w.	-19.5 (br, s), -42.5(br, s) (at 25°C); 8.9 (P_1) (d, $J(P_1–P_4)$ 93); -37.7 (P_2) (br, t, $J(P_2–P_3)$ 97), $J(P_2–P_4)$ 94); -45.8 (P_3) (d, $J(P_3–P_2)$ 97); -49.8 (P_4) (br, t, $J(P_4–P_1)$ 93, $J(P_4–P_2)$ 94) (at -95°C).
dppa		43.8 (s)
$[Ir_4(CO)_{10}(dppa)]$ (**3**)	2070 s, 2041 m, 2012 vs, 1980 m, 1860 w, 1825 m, 1778 m.	-17.1 (s) (at 25 and -95°C)
$[Ir_4(CO)_8(dppa)_2]$ (**4**)	2008 s, 1975 s(br), 1957 s, 1835 w, 1780 m, 1765 m.	0.3 (br, s), -12.4 (br, s) (at 25°C)

[a] CH_2Cl_2 solvent.

[b] Chemical shifts with respect to H_3PO_4 as external references; CH_2Cl_2 used as solvent; all coupling constants given in Hz; br, broad; s, singlet; d, doublet; dd, doublet of doublets; t, triplet.

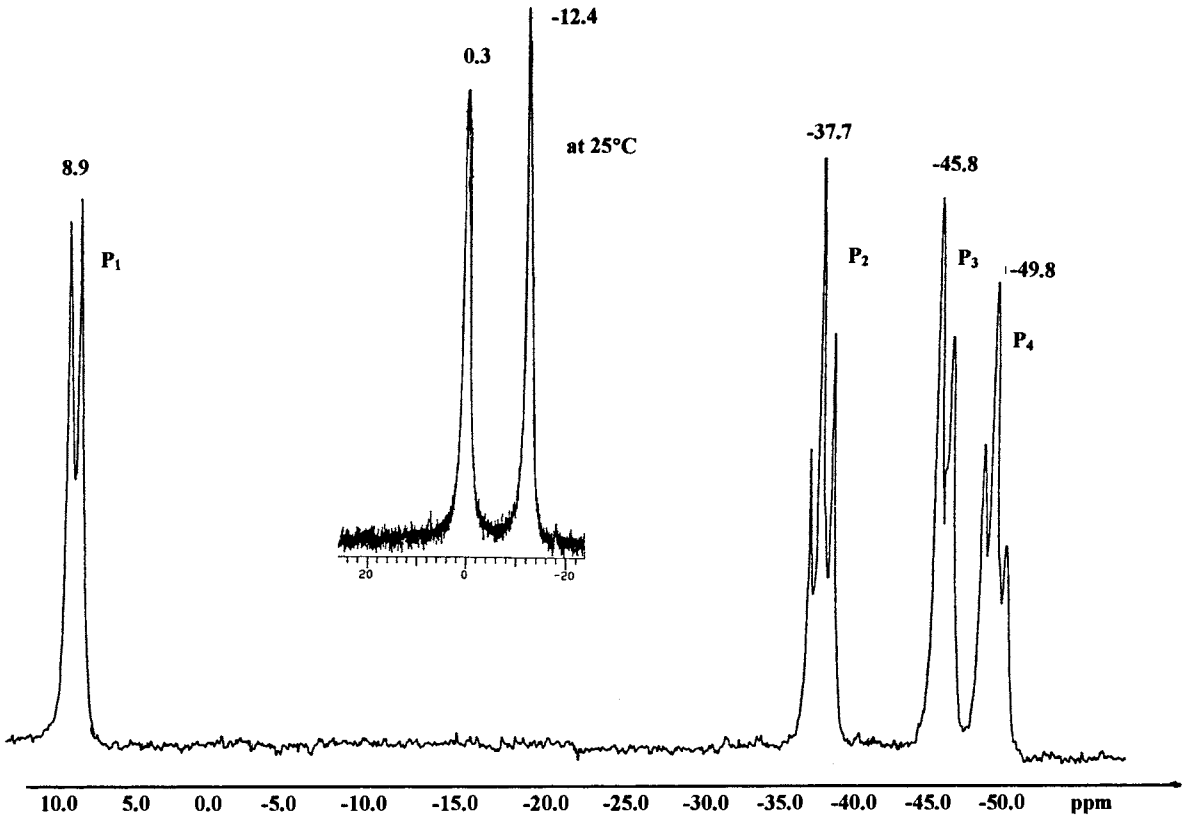

Fig. 1. The ^{31}P-NMR spectra of cluster complexes $[Ir_4(CO)_8(dppen)_2]$ (**2**) at −95°C and $[Ir_4(CO)_8(dppa)_2]$ (**4**) at 25°C.

NMR spectrum at room temperature (r.t.). These are because fluxionality is observed in $[Ir_4(CO)_8(dppen)_2]$ (**2**) or $[Ir_4(CO)_8(dppa)_2]$ (**4**). When the ^{31}P-NMR spectrum was run at a lower temperature (−95°C) two sharp doublets and two broadened triplets, which should be doublet of doublet, were observed. The spectrum can be represented as shown in Fig. 1. The ^{31}P-NMR spectroscopic data for complexes **2** or **4** (Table 1) suggest that each two phosphorus atoms in the same bidentate ligand are in similar chemical environments. This leads us to suggest that one of the bidentate phosphine ligand (P_1 and P_2) is coordinated at the diaxial sites and is bridged the Ir(1)–Ir(2). The second bidentate phosphine ligand (P_3 and P_4) would lead to a ^{31}P-NMR chemical shift difference. It occupies the radial site of the Ir(3) and the unique apical Ir(4) atom. It was found that when apical substitution occurs, basal phosphines rearrange to one radial and two axial groups [1,18]. Therefore, the AA′XX′ system that arises from complexes **2** gives a spectrum (Fig. 1) that allows phosphorus–phosphorus coupling to be obtained directly. The spectrum of the cluster complex **2** shows that all the phosphorus atoms are coordinated. It displays four sets of resonances. At 8.9 and −45.8 ppm, there are two doublets corresponding to the two phosphorus atoms P_1 and P_3 bound to Ir_1 and Ir_4, which result from phosphorus–phosphorus coupling with coupling constants $J(P_1P_4)$ 93 and $J(P_3P_2)$ 97 Hz, respectively. A resonance at −37.7 and −49.8 ppm (a shift of −34.3 or −46.4 ppm from free dppen ligand (−3.4 ppm)), due to the phosphorus atoms coordinated to the iridium metal framework, consists of a broadened triplet, which results from phosphorus–phosphorus coupling with coupling constants $J(P_4P_1)$ 93, $J(P_3P_2)$ 97 and $J(P_2P_4)$ 94 Hz. The two resonances at −45.8 and −49.8 ppm appear at lower field than that of the diaxial phosphorus P_1 and P_2 from dppen coordinated to the iridium metal framework. The present results are in agreement with those previously reported [6,7,18]. The FAB mass spectra of $[Ir_4(CO)_8(dppen)_2]$ (**2**) or $[Ir_4(CO)_8(dppa)_2]\cdot 3(THF)$ (**4**) show a parent ion at m/z 1786 or m/z 1763 as expected, respectively. The stepwise loss of eight carbonyl groups is also observed. The mass spectrum of the cluster complex **4** did not give a molecular ion peak at the desired position of m/z 1980. There is a difference of 217 amu, indicating the loss of three THF molecules. This result supported by the X-ray crystallographic determination of the cluster iridium complex **4**.

The X-ray crystal structure of the disubstituted species $[Ir_4(CO)_8(dppa)_2]\cdot 3(THF)$ (**4**) was determined. A perspective view of one molecule drawn to illustrate the mutual disposition of the bridging ligands is shown in Fig. 2. A listing of the selected bond distances and

angles is given in Table 2. The molecule consists of a tetrahedral core of iridium atoms, with the two dppa ligands coordinated in a bridging mode such that one carbonyl group on each Ir atom has been replaced by a phosphine. The geometry of this skeleton is better illustrated in Fig. 3, where phenyl groups have been removed and the stereochemistry of the remaining atoms emphasized. It is clear that the cluster iridium complex has the usual tetrahedral arrangement of iridium atoms. Three carbonyl groups are bridged to basal iridium atoms, which have two bridged dppa ligands. One dppa ligand was found to be bridged Ir(1) and Ir(2) and the other dppa ligand bridged Ir(3) and Ir(4) atoms. Relevant differences have been detected in bond distances between iridium atoms having bridged- or linearly-bonded carbonyl groups (e.g. Ir(1)–C(106) 2.171(12) and Ir(1)–C(101) 1.877(14) Å). The Ir–Ir bond lengths range from 2.6845(9) to 2.7498(8) Å, typical values for phosphine substituted tetrahedral iridium carbonyl clusters [4,23], and slightly longer than the average determined in the parent $[Ir_4(CO)_{12}]$ cluster (2.693) Å [24]. It may be significant that the shortest Ir–Ir bond, Ir(1)–Ir(2), is between the Ir atoms that are bridged by both the carbonyl group and the dppa ligand. This feature was also observed in the analogous iridium complex $[Ir_4(CO)_8(dppm)_2]$. Also, there is slight asymmetry (only possibly significant) in the bridging carbonyl groups (Ir(1)–C(104) 2.054(11), Ir(2)–C(104) 2.143(13); Ir(1)–C(106) 2.171(12), Ir(3)–C(106) 2.066(12); Ir(2)–C(105) 2.040(13), Ir(3)–C(105) 2.172 (12) Å). It may be significant that the bidentate phosphine ligand dppa is constrained to coordinate at axial sites in the basal plane of the Ir_4 tetrahedron, whereas in $[Ir_4(CO)_9(PPh_2Me)_3]$, which adopts the carbonyl-bridging C_{3v} structure, the phosphine ligands occupy one basal-axial and two basal-equatorial sites [25]. The average P–N bond distances of P(1)–N(1) 1.707(9); P(2)–N(1) 1.680(9); P(3)–N(2) 1.703(9) and P(4)–N(2) 1.674(8) are normal P–N bond distances [26]. One of the most notable features for the cluster complex **4** is the twisted configuration of one dppa ligand. The phosphorus atoms P(3) and P(4) are tilted away from the plane of Ir(2)–Ir(3)–Ir(4) triangle, forcing P(3) below and P(4) above the plane of the metal triangle. This favored conformation of the five-membered ring contributes to the tilting of the axial carbonyl ligands away from the precise positions.

3. Experimental

All reactions and manipulations of the new compounds were performed under a nitrogen or argon atmosphere, unless otherwise stated, using dry, degassed solvents and standard Schlenk-line techniques. IR spectra were recorded as dichloromethane (CH_2Cl_2) solutions in 0.5 mm NaCl solution cells. The $^{31}P\{^1H\}$-NMR spectra were obtained on JEOL FX-60 or Bruker WM250 instruments. The chemical shifts are relative to 85% H_3PO_4. Microanalyses were carried out in the Department of Chemistry, Liverpool University, UK. FAB mass spectra were recorded on a VG 7070E spectrometer. The compounds $Ph_2PC(=CH_2)PPh_2$ [27], $Ph_2PN(H)PPh_2$ [28] and $[Ir_4(CO)_{12}]$ [29] were prepared according to published procedures.

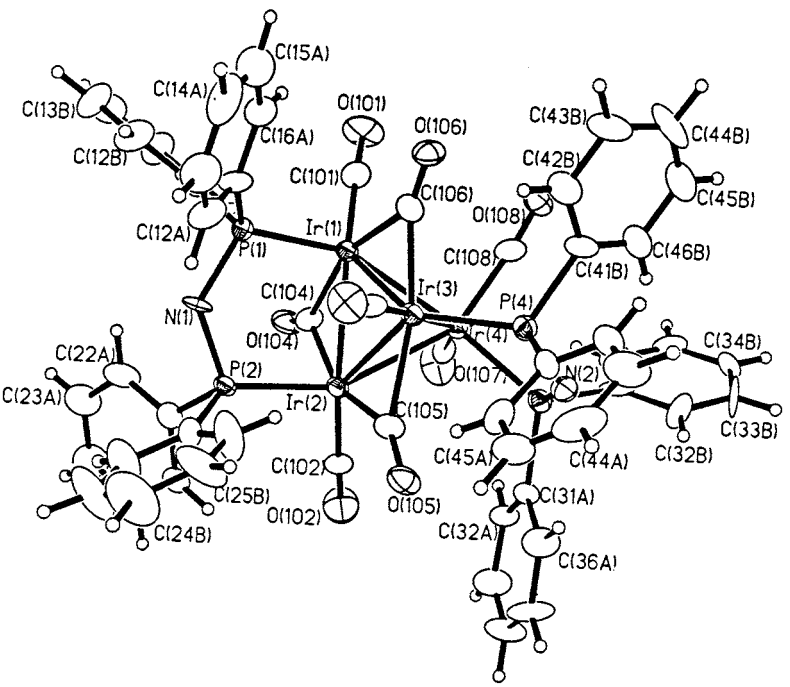

Fig. 2. Perspective drawing of $[Ir_4(CO_8(dppa)_2]\cdot 3(THF)$ (**4**) with ellipsoids drawn at the 40% probability level.

Table 2
Selected bond distances (Å) and angles (°) for $[Ir_4(CO_8(dppa)_2]\cdot 3(THF)$ (**4**)

Bond distances			
Ir(1)–C(101)	1.877(14)	C(101)–O(101)	1.132(14)
Ir(1)–C(104)	2.054(11)	C(102)–O(102)	1.119(13)
Ir(1)–C(106)	2.171(12)	C(103)–O(103)	1.153(14)
Ir(1)–P(1)	2.271(3)	C(104)–O(104)	1.148(14)
Ir(1)–Ir(2)	2.6845(9)	C(105)–O(105)	1.162(14)
Ir(1)–Ir(4)	2.7110(8)	C(106)–O(106)	1.133(13)
Ir(1)–Ir(4)	2.7366(10)	C(107)–O(107)	1.128(14)
Ir(2)–C(102)	1.875(11)	C(108)–O(108)	1.128(14)
Ir(2)–C(105)	2.040(13)	P(1)–N(1)	1.707(9)
Ir(2)–C(104)	2.143(13)	P(1)–C(11A)	1.801(11)
Ir(2)–P(2)	2.300(3)	P(1)–C(11b)	1.855(12)
Ir(2)–Ir(4)	2.7323(11)	P(2)–N(1)	1.680(9)
Ir(2)–Ir(3)	2.7498(8)	P(2)–C(21b)	1.836(13)
Ir(3)–C(103)	1.858(11)	P(2)–C(21A)	1.836(12)
Ir(3)–C(106)	2.066(12)	P(3)–N(2)	1.703(9)
Ir(3)–C(105)	2.172(12)	P(3)–C(31A)	1.833(11)
Ir(3)–P(4)	2.252(3)	P(3)–C(31B)	1.837(13)
Ir(4)–Ir(4)	2.7175(11)	P(4)–N(2)	1.674(8)
Ir(4)–C(108)	1.886(13)	P(4)–C(41A)	1338(13)
Ir(4)–C(107)	1.902(12)	P(4)–C(41B)	1.842(12)
Ir(4)–P(3)	2.289(3)		
Bond angles			
C(101)–Ir(1)–C(104)	101.8(5)	C(102)–Ir(2)–P(2)	100.6(4)
C(101)–Ir(1)–C(106)	94.3(5)	C(105)–Ir(2)–P(2)	104.6(3)
C(104)–Ir(1)–C(106)	159.0(5)	C(104)–Ir(2)–P(2)	86.1(3)
C(101)–Ir(1)–P(1)	99.2(4)	C(102)–Ir(2)–Ir(1)	141.6(4)
C(104)–Ir(1)–P(1)	92.4(3)	C(105)–Ir(2)–Ir(1)	111.8(3)
C(106)–Ir(1)–P(1)	98.3(3)	C(104)–Ir(2)–Ir(1)	48.8(3)
C(101)–Ir(1)–Ir(2)	150.7(3)	P(2)–Ir(2)–Ir(1)	93.68(7)
C(104)–Ir(1)–Ir(2)	51.7(4)	C(102)–Ir(2)–Ir(4)	102.5(4)
C(106)–Ir(1)–Ir(2)	109.1(3)	C(105)–Ir(2)–Ir(4)	84.5(3)
P(1)–Ir(1)–Ir(2)	94.75(8)	C(104)–Ir(2)–Ir(4)	72.6(3)
C(101)–Ir(1)–Ir(4)	107.2(4)	P(2)–Ir(2)–Ir(4)	153.57(7)
C(104)–Ir(1)–Ir(4)	80.5(3)	Ir(1)–Ir(2)–Ir(4)	60.06(2)
C(106)–Ir(1)–Ir(4)	81.9(3)	C(102)–Ir(2)–Ir(3)	143.5(4)
P(1)–Ir(1)–Ir(4)	153.52(8)	C(105)–Ir(2)–Ir(3)	51.4(3)
Ir(2)–Ir(1)–Ir(4)	60.85(3)	C(104)–Ir(2)–Ir(3)	108.8(3)
C(101)–Ir(1)–Ir(3)	139.5(4)	P(2)–Ir(2)–Ir(3)	106.92(7)
C(104)–Ir(1)–Ir(3)	112.2(4)	Ir(1)–Ir(2)–Ir(3)	60.46(3)
C(106)–Ir(1)–Ir(3)	48.1(3)	Ir(4)–Ir(2)–Ir(3)	59.43(3)
P(1)–Ir(1)–Ir(3)	100.62(8)	C(103)–Ir(3)–C(106)	96.7(5)
Ir(2)–Ir(1)–Ir(3)	60.95(2)	C(103)–Ir(3)–C(105)	96.1(4)
Ir(4)–Ir(1)–Ir(3)	59.85(3)	C(106)–Ir(3)–C(105)	157.2(5)
C(102)–Ir(2)–C(105)	98.8(5)	C(103)–Ir(3)–P(4)	96.6(4)
C(102)–Ir(2)–C(104)	96.6(5)	C(106)–Ir(3)–P(4)	101.00)
C(105)–Ir(2)–C(104)	159.2(5)	C(105)–Ir(3)–P(4)	96.2(4)
C(103)–Ir(3)–Ir(4)	176.3(4)	C(107)–Ir(4)–Ir(3)	152.1(4)
C(106)–Ir(3)–Ir(4)	83.6(3)	P(3)–Ir(4)–Ir(3)	91.33(8)
C(105)–Ir(3)–Ir(4)	82.5(3)	Ir(1)–Ir(4)–Ir(3)	60.55(3)
P(4)–Ir(3)–Ir(4)	87.03(7)	C(108)–Ir(4)–Ir(2)	150.0(3)
C(103)–Ir(3)–Ir(1)	117.7(4)	C(107)–Ir(4)–Ir(2)	92.1(4)
C(106)–Ir(3)–Ir(1)	51.5(3)	P(3)–Ir(4)–Ir(2)	106.50(8)
C(105)–Ir(3)–Ir(1)	105.8(3)	Ir(1)–Ir(4)–Ir(2)	59.10(2)
P(4)–Ir(3)–Ir(1)	136.11(8)	Ir(3)–Ir(4)–Ir(2)	60.60(2)
Ir(4)–Ir(3)–Ir(1)	59.61(3)	O(101)–C(101)–Ir(1)	177.4(12)
C(103)–Ir(3)–Ir(2)	116.6(3)	O(102)–C(102)–Ir(2)	175.3(12)
C(106)–Ir(3)–Ir(2)	110.0(3)	O(103)–C(103)–Ir(3)	176.2(11)
C(105)–Ir(3)–Ir(2)	47.2(3)	O(104)–C(104)–Ir(1)	142.2(10)
P(4)–Ir(3)–Ir(2)	130.19(7)	O(104)–C(104)–Ir(2)	138.3(9)
Ir(4)–Ir(3)–Ir(2)	59.96(3)	Ir(1)–C(104)–Ir(2)	79.5(4)
Ir(1)–Ir(3)–Ir(2)	58.59(3)	O(105)–C(105)–Ir(2)	142.7(9)
C(108)–Ir(4)–C(107)	101.1(5)	O(105)–C(105)–Ir(3)	135.8(9)
C(108)–Ir(4)–P(3)	96.8(4)	Ir(2)–C(105)–Ir(3)	81.5(5)
C(107)–Ir(4)–P(3)	102.6(4)	O(106)–C(106)–Ir(3)	143.6(10)
C(108)–Ir(4)–Ir(1)	91.6(4)	O(106)–C(106)–Ir(1)	135.9(10)
C(107)–Ir(4)–Ir(1)	102.2(3)	Ir(3)–C(106)–Ir(1)	80.4(4)
P(3)–Ir(4)–Ir(1)	151.76(8)	O(107)–C(107)–Ir(4)	179.0(11)
C(108)–Ir(4)–Ir(3)	101.1(3)	O(108)–C(108)–Ir(4)	174.8(12)

3.1. Preparation of $[Ir_4(CO)_{10}(dppen)]$ (**1**) or $[Ir_4(CO)_{10}(dppa)]$ (**3**)

$[Ir(CO)_2Cl(p\text{-toluidine})]$ (1.063 g, 2.72 mmol), dppen (0.2702 g, 0.68 mmol), or dppa (0.2627 g, 0.68 mmol), acid-washed mossy zinc (9.0 g), 2-methoxyethanol (150 cm^3), and water (6 cm^3) were placed in a 500 cm^3 heavy-walled glass pressure vessel. The mixture was saturated with CO and then pressurized to 4 atm with CO. The reaction vessel was heated to 90°C for 45 min, with stirring, and then cooled, vented, and the solution filtered under nitrogen. The filtrate was reduced in volume and chromatography on Florisil using a 5:1 petroleum ether–dichloromethane eluant. Two bands were collected, a yellow band of $[Ir_4(CO)_{10}(dppen)]$ or $[Ir_4(CO)_{10}(dppa)]$, followed by an orange band of $[Ir_4(CO)_8(dppen)_2]$ or $[Ir_4(CO)_8(dppa)_2]$. The yellow product was recrystallised from THF–hexane to give yellow crystals of $[Ir_4(CO)_{10}(dppen)]$ (**1**) (66 mg, 6.7%). Found: C, 29.65; H, 1.48. $Ir_4C_{36}H_{22}O_{10}P_2$. Calc.: C, 29.92; H, 1.53%. $m/z = 1445$ (mass spectrometry) as required for $[Ir_4(CO)_{10}(Ph_2PC(=CH_2)PPh_2)]$; and $[Ir_4(CO)_{10}(dppa)]$ (**3**) (80 mg, 8.2%) Found: C, 28.32; H, 1.45; N, 0.88. $Ir_4C_{34}H_{21}O_{10}P_2N$. Calc.: C, 28.47; H, 1.48; N, 0.98%. $m/z = 1435$ (mass spectrometry) as required for $[Ir_4(CO)_{10}(Ph_2PN(H)PPh_2)]$; $[Ir_4(CO)_8(dppen)_2]$ (**2**) (0.14 g, 14%). Found: C, 41.12; H, 2.55. $Ir_4C_{60}H_{52}O_8P_4$. Calc.: C, 41.48; H, 2.86%. $m/z = 1183$ (mass spectrometry) as required for $[Ir_4(CO)_8(Ph_2PC(=CH_2)PPh_2)_2]$; or $[Ir_4(CO)_8(dppa)_2]$ (**4**) (0.129 g, 14.8%). Found: C, 41.11; H, 3.45; N, 1.35. $Ir_4C_{68}H_{66}O_{11}P_4N_2$. Calc.: C, 41.25; H, 3.36; N, 1.41%. $m/z = 1980$ (mass spectrometry) as required for $[Ir_4(CO)_8(Ph_2PN(H)\ PPh_2)_2]\cdot 3(C_4H_8O)$.

3.2. Preparation of $[Ir_4(CO)_8(dppen)_2]$ (**2**) or $[Ir_4(CO)_8(dppa)_2]$ (**4**)

$[Ir_4(CO)_{12}]$ (0.282 g, 0.28 mmol) and dppen (0.224 g, 0.56 mmol) or dppa (0.218 g, 0.56 mmol) in toluene (30 cm^3) were heated under reflux for 3 h. The resulting orange–red solution was filtered and evaporated to dryness under reduced pressure to give an orange solid. Recrystallization from THF–hexane gave orange crystals of $[Ir_4(CO)_8(dppen)_2]$ (**2**) (0.35 g, 34.7%) or $[Ir_4(CO)_8(dppa)_2]$ (**4**) (0.45 g, 45%).

3.3. X-ray crystallography procedures

3.3.1. General information

Orange crystals of the cluster complex $[Ir_4(CO)_8(dppa)_2]\cdot 3(THF)$ suitable for X-ray diffraction studies were obtained. The basic crystallographic procedures used have been fully described elsewhere [30,31]. Data sets were collected, corrected for Lorentz, polarization, absorption effects, and merged. The positions of the Ir and P atoms were given by a Patterson superposition method. The remainder of the atoms were found in subsequent sets of least-squares refinement cycles, followed by difference Fourier maps using the SHELX-93 structure refinement program [32]. All calculations were performed on a DEC 3000-800 AXP workstation. A listing of the selected bond distances and angles for $[Ir_4(CO)_8(dppa)_2]\cdot 3(THF)$ is presented in Table 2. It was found that two fully occupied sites containing THF molecules were located, as were two other approximately half-occupied sites. Hydrogen atoms were added to the model in calculated positions for the phenyl groups of the metal cluster complex. In the final refinement cycles, all the non-hydrogen atoms of the metal complex were given anisotopic displacement parameters, as were the atoms on the two fully occupied THF sites.

3.3.2. Crystal structure analysis of $[Ir_4(CO)_8(dppa)_2]\cdot 3(THF)$ (**4**)

Orange crystals of the cluster complex $[Ir_4(CO)_8(dppa)_2]\cdot 3(THF)$ were grown from a THF–hexane solution. The crystals were sensitive to solvent loss and thus a suitable crystal of dimensions of $0.40 \times 0.25 \times 0.18$ mm was attached to the tip of a quartz fiber with a small amount of grease and immediately transferred into a low-temperature stream of nitrogen (-100°C) on an Enraf–Nonius CAD-4S diffractometer equipped with graphite monochromator and Mo–K_α ($\lambda = 0.71073$ Å) radiation. Reflections (250) in the range 9.0–20.1 θ were centered to refine the reduced parameters corresponding to the triclinic crystal system. A total of 8979 data were collected using an ω scan technique. Full refinement of 797 parameters led to residuals of $R = 0.052$ (for 8971 reflections with $I > 2\sigma(I)$) and $R = 0.062$ (for all 8979 data).

3.3.3. Crystal data

$C_{68}H_{66}Ir_4N_2O_{11}P_4$, $M = 1979.91$, triclinic, space group $P\bar{1}$, $a = 12.452(3)$, $b = 16.181(3)$, $c = 17.806(4)$ Å, $\beta = 89.01(3)°$, $V = 3545.4(12)$ Å^3, $Z = 2$, $D_{calc} = 1.855$ g cm^{-3}, $\mu = 7.63$ mm^{-1}, $T = -60$°C, $R = 0.052$ (for 8971 reflections with $I > 2\sigma(I)$) and $R_{int} = 0.000$ (for all 8979 data).

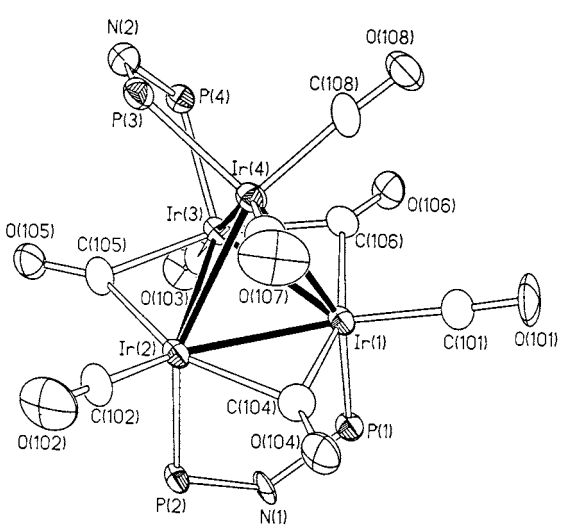

Fig. 3. Thermal ellipsoid plot of the molecule with the phenyl groups removed.

4. Supplementary material

Crystallographic data for the structure analysis have been deposited with the Cambridge Crystallographic Data Centre, CCDC no. 139261 for the compound $[Ir_4(CO_8(dppa)_2]\cdot 3(THF)$. Copies of this information may be obtained free of charge from The Director, CCDC, 12 Union Road, Cambridge CB2 1EZ, UK (fax: +44-1223-336033 or e-mail: deposit@ccdc.cam.ac.uk or www: http://www.ccdc.cam.ac.uk).

Acknowledgements

We thank Dr Lee M. Daniels (Laboratory for Molecular Structure and Bonding, Texas A&M University) for the diffraction data collection.

References

[1] F.H. Carré, F.A. Cotton, B.A. Frenz, Inorg. Chem. 15 (1976) 380.
[2] J. Evans, B.P. Gracey, L.R. Gray, M. Webster, J. Organomet. Chem. 240 (1982) C61.
[3] D.F. Foster, J. Harrison, B.S. Nicholls, A.K. Smith, J. Organomet. Chem. 248 (1983) C29.
[4] M.M. Harding, B.S. Nicholls, A.K. Smith, Acta Crystallogr. Sect. C 40 (1984) 790.
[5] D.F. Foster, J. Harrison, B.S. Nicholls, A.K. Smith, J. Organomet. Chem. 295 (1985) 99.
[6] N. Nawar, J. Chem. Res. (s) (1994) 498.
[7] N. Nawar, A.K. Smith, Inorg. Chim. Acta 227 (1994) 79.
[8] P. Braunstein, Actual. Chim. 7 (1996) 75.
[9] P. Braunstein, J.R. Galsworthy, B.J. Hendan, H.C. Marsmann, J. Organomet. Chem. 551 (1998) 125.
[10] M.H. Araujo, P.B. Hitchcock, J.F. Nixon, M.D. Vargas, J. Braz. Chem. Soc. 9 (1998) 563.
[11] R. Whyman, Transition Metal Clusters, Wiley, New York, 1980, Ch. 8.
[12] A.K. Smith, J.M. Basset, J. Mol. Catal. 2 (1977) 229.

[13] G. Balavoine, J. Collin, J.J. Bonnet, G. Lavigne, J. Organomet. Chem. 280 (1985) 429.
[14] P. Braunstein, T. Faure, M. Knorr, T. Staehrfeldt, A. DeCian, J. Fischer, Gazz. Chim. Ital. 125 (1995) 35.
[15] P. Braunstein, C. Graiff, X. Morise, A. Tiripicchio, J. Organomet. Chem. 541 (1997) 417.
[16] P. Bhattacharyya, J.D. Woollins, Polyhedron 14 (1995) 3367.
[17] J. Ellermann, K.J. Meier, Z. Anorg. Chem. 603 (1991) 77.
[18] K.J. Karel, J.R. Norton, J. Am. Chem. Soc. 96 (1974) 6812.
[19] G.F. Stuntz, J.R. Shapley, Inorg. Chem. 15 (1976) 1994. [20] D.F. Foster, B.S. Nicholls, A.K. Smith, J. Organomet. Chem. 236 (1982) 395.
[21] J.R. Shapley, G.F. Stuntz, M.R. Churchill, J.P. Hutchinson, J. Am. Chem. Soc. 101 (1979) 7425.
[22] M.I. Bruce, G. Shaw, F.G.A. Stone, J. Chem. Soc. Dalton Trans. (1972) 2094.
[23] D.J. Darensbourg, B.J. Baldwin-Zuschke, Inorg. Chem. 20 (1981) 2846.
[24] M.R. Churchill, J.P. Hutchinson, Inorg. Chem. 17 (1978) 3528.
[25] P.E. Cattermole, K.G. Orrell, A.G. Osborne, J. Chem. Soc. Dalton Trans. (1974) 238.
[26] N. Nawar, J. Organomet. Chem. (in press).
[27] H. Schmidbaur, R. Herr, J. Riede, Chem. Ber. 117 (1984) 2322.
[28] H. Noeth, L. Meinel, Z. Anorg. Chem. 349 (1967) 225.
[29] L. Malatesta, G. Caglio, Chem. Commun. (1967) 420.
[30] F.A. Cotton, E.V. Dikarev, W.Y. Wong, Inorg. Chem. 30 (1997) 80.
[31] F.A. Cotton, E.V. Dikarev, N. Nawar, W.Y. Wong, Inorg. Chem. 36 (1997) 559.
[32] G.M. Sheldrick, in: H.D. Flack, L. Parkanyi, K. Simon (Eds.), Crystallographic Computing 6, Oxford University Press, Oxford, 1993, p. 111.